View metadata, citation and similar papers at core.ac.uk

brought to you by CORE

provided by Online Research Database In Technology

Technical University of Denmark

Structural defects and epitaxial rotation of C-60 and C-70(111) films on GeS(001)

Bernaerts, D.; Van Tendeloo, G.; Amelinckx, S.; Hevesi, K.; Gensterblum, G.; Yu, L.M.; Pireaux, J.-J.; Grey, Francois; Bohr, Jakob

Published in:
Journal of Applied Physics

Link to article, DOI:
10.1063/1.363241

Publication date:
1996

Document Version
Publisher's PDF, also known as Version of record

Link back to DTU Orbit

Citation (APA):
Bernaerts, D., Van Tendeloo, G., Amelinckx, S., Hevesi, K., Gensterblum, G., Yu, L. M., ... Bohr, J. (1996). Structural defects and epitaxial rotation of C-60 and C-70(111) films on GeS(001). Journal of Applied Physics, 80(6), 3310-3318. DOI: 10.1063/1.363241

DTU Library
Technical Information Center of Denmark

General rights
Copyright and moral rights for the publications made accessible in the public portal are retained by the authors and/or other copyright owners and it is a condition of accessing publications that users recognise and abide by the legal requirements associated with these rights.

- Users may download and print one copy of any publication from the public portal for the purpose of private study or research.
- You may not further distribute the material or use it for any profit-making activity or commercial gain
- You may freely distribute the URL identifying the publication in the public portal

If you believe that this document breaches copyright please contact us providing details, and we will remove access to the work immediately and investigate your claim.

Structural defects and epitaxial rotation of C_{60} and C_{70}(111) films on GeS(001)

D. Bernaerts,[a] G. Van Tendeloo, and S. Amelinckx
EMAT, University of Antwerp RUCA, Groenenborgerlaan 171, B 2020 Antwerp, Belgium

K. Hevesi, G. Gensterblum, L. M. Yu, and J.-J. Pireaux
Laboratoire Interdisciplinaire de Spectroscopie Electronique, Institute for Studies in Interface Sciences, Facultés Universitaires Notre-Dame de la Paix, B-5000 Namur, Belgium

F. Grey and J. Bohr
Technical University of Denmark, DK 2800 Lyngby, Denmark

(Received 30 April 1996; accepted for publication 11 June 1996)

A transmission electron microscopy study of epitaxial C_{60} and C_{70} films grown on a GeS (001) surface is presented. The relationship between the orientation of the substrate and the films and structural defects in the films, such as grain boundaries, unknown in bulk C_{60} and C_{70} crystals, are studied. Small misalignments of the overlayers with respect to the orientation of the substrate, so-called epitaxial rotations, exist mainly in C_{70} films, but also sporadically in the C_{60} overlayers. A simple symmetry model, previously used to predict the rotation of hexagonal overlayers on hexagonal substrates, is numerically tested and applied to the present situation. Some qualitative conclusions concerning the substrate-film interaction are deduced. © *1996 American Institute of Physics.* [S0021-8979(96)04518-5]

I. INTRODUCTION

Investigation of solid state properties of fullerenes[1,2] requires high quality crystalline materials which could not be easily achieved. Therefore the heteroepitaxial growth of fullerene films attracted much interest. Several substrates have been used: metallic single crystals, conventional, and layered semiconducting materials. Metallic substrates yielded single-domain epitaxy [Cu(111),[3–5] Au(110),[6] and Ni(110)[7]] or multidomain epitaxy [Au(111),[8–10] Ag(111),[8] Cu(100),[3] and Cu(110)[3]] of C_{60}. Depending on the lattice mismatch and on the strength of the interface interaction, the films consist in strained or deformed hexagonal monolayers[6,11] sometimes leading to changes in the substrate surface reconstruction.[8,10] Due to the high step density of the metal surfaces, the domain size of the overlayers is limited to a few tens of nanometers.[3,8] Si and GaAs are the two conventional semiconductors used for growing fullerene films and although the step density is much lower, only multidomain[12–15] or small-grain crystalline[16–18] islands could be grown. Heating the substrate resulted in well-ordered films with domain sizes exceeding 100 nm.[15,17,19,20] The best crystalline quality was obtained for films grown on lamellar substrates like GeS(001),[18,21] GaSe(0001),[22,23] MoS_2(0001),[22,24–26] and mica(001).[27–31] The low surface energy of these materials and the absence of unsaturated chemical bonds at their surface relax the lattice matching conditions required for epitaxial growth and favor surface diffusion of the deposited molecules. The surfaces of these layered materials show up as large terraces with low step density allowing the growth of very large islands up to 1 μm in diameter for C_{60} on MoS_2.[28] The GeS(001) crystal seems particularly adequate for C_{60} film growth with a lattice mismatch of about 0.9%[18] while C_{70} is at its best on MoS_2[26] or mica.[31]

Structural studies have shown crystalline defects of fullerenes films lifted from the mica(001)[31–33] or MgO(001)[34] substrate surface. However, lifting the films hinders the investigation of the role of the substrate. Beyond the grain boundaries caused by substrate surface steps,[35] the influence of the substrate is very important to explain stacking faults. The energy difference between fcc and hcp packing is so small that the least lattice misfit or deposit perturbation might cause stacking faults.[31]

This work presents a high resolution transmission electron microscopy (HREM) study of fullerene films on GeS(001) and investigates the relationship between the lattice mismatch and the observed epitaxial rotations. Although epitaxial C_{60}(111)/GeS(001) have been reported to be single crystalline,[21] the present HREM experiments show the occasional presence of epitaxial rotations. Similar epitaxial rotations are more frequently observed in C_{70} epitaxial films due to the larger lattice mismatch (about 6.4%). The observed rotation angles can be explained by a simple symmetry model developed by Grey *et al.*[36]

II. EXPERIMENT

HPLC purified C_{60}(>99.9%) and C_{70}(>98%) powders (MER Corp., Tucson, AZ) were loaded in a Knudsen cell which had been outgassed at 450 °C for 12 h prior to deposition. The basic pressure in the chamber was 1×10^{-9} Torr. The fullerenes were then sublimated (~420 °C) onto a freshly *in situ* cleaved GeS(001) single crystal (GeS temperature ~180 °C). An outstanding crystallographic quality was observed by LEED for the clean substrate and for the thin and thick C_{60} films; the LEED patterns were diffuse for the C_{70} films.[21,37] Preparation of the samples for TEM was done

[a]Electronic mail: diber@ruca.ua.ac.be

 0021-8979/96/80(6)/3310/9/$10.00 © 1996 American Institute of Physics

Downloaded¬05¬Aug¬2009¬to¬192.38.67.112.¬Redistribution¬subject¬to¬AIP¬license¬or¬copyright;¬see¬http://jap.aip.org/jap/copyright.jsp

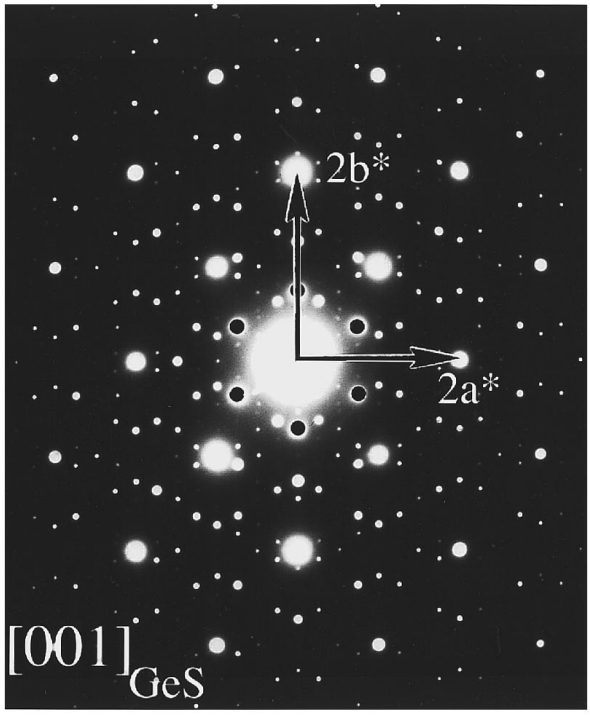

FIG. 1. Selected area electron diffraction pattern of a 20 nm thick C_{60} film on a GeS (001) surface, taken along the [001]-zone of GeS. The black dots indicate the hexagonal structure of the C_{60} [111] pattern around the central spot.

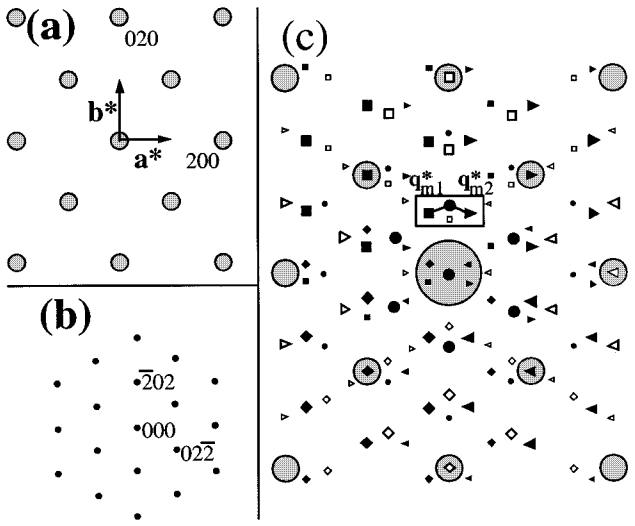

FIG. 2. (a) Schematic [001] diffraction pattern of GeS. (b) Schematic [111] pattern of C_{60}. (c) Schematic pattern of a C_{60} overlayer on GeS (001). On every GeS spot the C_{60} [111] pattern is superposed.

by polishing and ion milling the substrate side of the sample until a small hole was formed. The resulting wedge-shaped crystal areas contain both the fullerene film and substrate. Only plan view samples were prepared. A Philips CM20 electron microscope (200 kV) was used for the observations. No special care was taken to protect the films from the influence of air, but the samples were stored as much as possible in the dark. Rusakova *et al.*[38] showed that only a combination of exposure to air and intense light has an influence on the structural properties of C_{60} and C_{70} films. Moreover, we did not observe the rapid amorphization of the films under influence of the electron beam, indicating the high purity of the films and the absence of changes caused by air or light.[38]

III. OBSERVATIONS

A. Diffraction experiments

1. C_{60}(111) overlayer on GeS(001)

Selected area electron diffraction (SAED) experiments make the determination of the orientation-relation between the adsorbate and the substrate possible for very small areas. A typical SAED-pattern for a C_{60} overlayer on a GeS(001) surface shown in Fig. 1, is observed with the electron beam normal to the substrate surface. The incoming electron beam is diffracted by the substrate (orthorhombic structure with $a=0{,}429$ nm, $b=0{,}364$ nm, and $c=1{,}047$ nm) according to the [001]* diffraction pattern of GeS [Fig. 2(a)] with the extinction conditions for the space group Pcmn (No. 62) of GeS (bright spots in Fig. 1). The diffracted beams act as incoming beams for the C_{60} crystal and are diffracted according to its [111]* pattern [Fig. 2(b)]. The result is a [001]* pattern of GeS, with the [111]* pattern of C_{60} superposed on every spot [Fig. 2(c)]. All the observed spots can readily be explained in this way.

The relation (in reciprocal coordinates) between the orientation of the overlayer and the substrate found from Fig. 1 is

$$C_{60}[111]^* \| \mathrm{GeS}[001]^*,$$

$$C_{60}[10\bar{1}]^* \| \mathrm{GeS}[0\bar{1}0]^*,$$

$$C_{60}[\bar{1}2\bar{1}]^* \| \mathrm{GeS}[100]^*,$$

confirming LEED experiments.[18,21] All observed diffraction patterns are consistent with the fcc-structure of C_{60}, with lattice constant $a_{C_{60}} = 1.41 \pm 0.02$ nm, corresponding to the lattice constant of bulk C_{60}. It has been observed that the very first monolayer of the C_{60} overlayer adopts its bulklike structure,[18] which is confirmed by our results. The ED-pattern of Fig. 1 was observed in all parts of the film, except in a few small, disordered, and rotated grains, indicating the good crystallinity of the film in regions with dimensions of the order of a micron or larger. The reason why the GeS(001) face is such a good template for a C_{60} overlayer was discussed previously.[18,21] The substrate lattice parameter in the *a*-direction (0.429 nm) matches very well half the distance between the [101] C_{60} rows (0.86 nm) of the close-packed overlayer. The GeS(001) surface can be considered as an arrangement of one-dimensional grooves, parallel to the *b* axis and with a periodicity of 0.429 nm. The [101] rows of C_{60} molecules can align with these one-dimensional grooves[39] and by systematically skipping every second, it is possible to complete the monolayer [Fig. 2 and Fig. 5 of Ref. 18). The accurate alignment of the film with respect to the substrate is clear from the symmetrical appearance of the set of spots indicated in Fig. 2(c) (equal length of $\mathbf{q}^*_{\mathbf{m1}}$ and $\mathbf{q}^*_{\mathbf{m2}}$).

Downloaded¬05¬Aug¬2009¬to¬192.38.67.112.¬Redistribution¬subject¬to¬AIP¬license¬or¬copyright;¬see¬http://jap.aip.org/jap/copyright.jsp

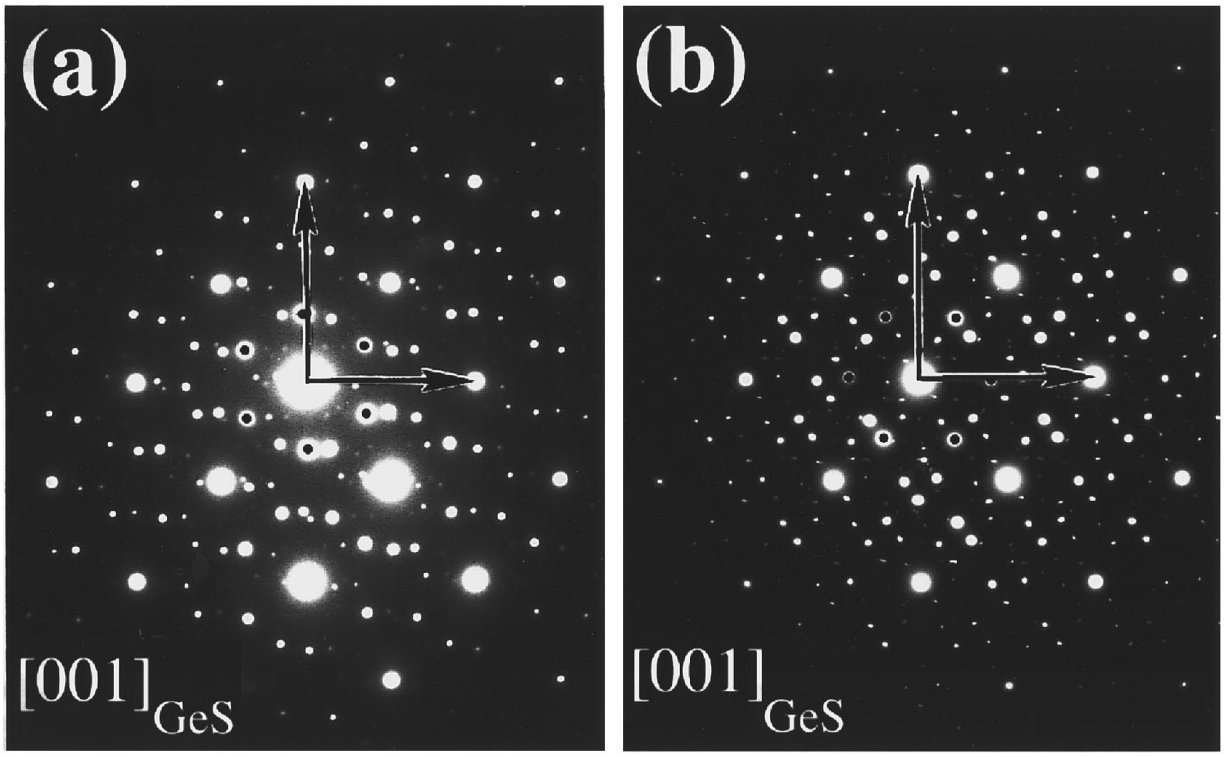

FIG. 3. Selected area electron diffraction patterns of a 20 nm thick C_{70} film on GeS (001), along the [001] direction of GeS. (a) Orientation I, (b) orientation II.

2. C_{70}(111) overlayer on GeS(001)

C_{70} molecules can align their long axis normal to the (001) GeS surface upon deposition, resulting in intermolecular distances (in the first monolayer) comparable to the C_{60}–C_{60} distance and we expect the same alignment of the overlayer with the substrate. Instead of fcc, the structure of the overlayer would be rhombohedral or hexagonal with a c/a larger than the ideal value.[40,41] Another possibility is that the molecules rotate isotropically and form a hcp or fcc crystal, with the C_{70}–C_{70} distance somewhat larger (1.05 nm). The misfit between $2a_{GeS}$ and the distance between the [101] C_{70} rows (0.91 nm) becomes larger, influencing epitaxy.

Typical ED patterns for a C_{70} overlayer on a GeS(001) surface are shown in Fig. 3, and are all consistent with a fcc structure, possibly with some stacking disorder in the (111) planes parallel to the surface. No indication for crystal parts with orientationally aligned C_{70} molecules was found, although we cannot completely exclude the presence of some monolayers with aligned molecules. The effect of the larger lattice $[a_{C_{70}} = (1.48 \pm 0.02)$ nm] parameter is clear in Fig. 3(a). Furthermore, $\mathbf{q}^*_{\mathbf{m1}}$ and $\mathbf{q}^*_{\mathbf{m2}}$ [indicated in Fig. 2(c)] are not equal in length, indicating that the overlayer is rotated about the surface normal over a small angle θ. However, since θ is small, the relation between the orientation of the film and the substrate as observed for C_{60} is still approximately valid. We will call this orientation I.

Patterns as in Fig. 3(b) were also observed for some C_{70} grains, consistent with a rotation of the C_{70} overlayer over θ=90° (or 30° which is an equivalent configuration for the first monolayer) about the normal to the substrate surface. This results in the following relations

$$C_{70}[111]^* \| GeS[001]^*,$$

$$C_{70}[\bar{1}2\bar{1}]^* \| GeS[0\bar{1}0]^*,$$

$$C_{70}[10\bar{1}]^* \| GeS[100]^*,$$

(orientation II). For this orientation the alignment with the substrate is not perfect either. Diffraction patterns along other zone axes show that the structure of the overlayer is also fcc with a lattice parameter $a_{C_{70}} = (1.49 \pm 0.02)$ nm and again no indication for the presence of orientationally aligned C_{70} molecules was found.

In some smaller parts of the film, other overlayer orientations were found; the rotation angles θ observed for different grains are listed in Table I. Angles in the complete 0°–30° range could be found from the ED patterns, although values for θ around 1° and especially around 2° were most frequently observed. In the C_{70} overlayer, large grains (of the order of at least one square micron) with a uniform orientation on the substrate are intermixed with smaller ones having other orientations, which explains the diffuse LEED patterns.

B. High resolution experiments

1. [111] zone of the overlayer

Figure 4(a) shows a HREM image of a perfectly crystalline part of a C_{60}(111) film on GeS(001), viewed along the

Downloaded¬05¬Aug¬2009¬to¬192.38.67.112.¬Redistribution¬subject¬to¬AIP¬license¬or¬copyright;¬see¬http://jap.aip.org/jap/copyright.jsp

TABLE I. Observed rotation angles θ for different C_{60} and C_{70} grains with respect to the orientation of the substrate, as determined from ED patterns and HREM images. $\theta=0$ was chosen for the configuration with rows of the closed packed molecules (the [101] rows) aligned with the grooves on the GeS surface parallel to the *b* axis. For C_{60} films, only rotation angles different from 0 are given.

C_{60}	C_{70}		
	0.0±0.3	1.1±0.4(2×)	5.1±0.4
5.2±0.5	0.1±0.4	1.2±0.4	12.8±0.4
14.7±0.5	0.2±0.4	1.8±0.4(2×)	13.1±0.5
15.6±0.5	0.3±0.4	2.0±0.4	14.7±0.5
	0.4±0.4(2×)	2.2±0.4(2×)	27.7±0.5
		2.3±0.4	28.0±0.5

[111] zone of the overlayer. The bright spots clearly reflect the sixfold symmetry of the close-packed (111) planes. In Ref. 42 it was mentioned that dark details in HREM images of fullerene crystals, taken at Scherzer defocus, correspond to electron-rich regions of the *projected* structure of the crystal. Bright image details can be identified as electron-poor regions, such as the centers of the spherical molecules. For the projection of a fcc crystal (...*ABC*... stacking) along the [111]-axis, we thus expect bright spots at the positions of the molecules of the first monolayer (*A*-type layer), as well as at the positions of the molecules of the *B* and the *C* layers. The resulting pattern is a hexagonal array of bright spots with a spacing of $\sqrt{6}/6a_{C_{60}} = 0.58$ nm. Although the structure of the substrate is not resolved in Fig. 4(a), its presence can be concluded from the moiré pattern. The direction of the corresponding moiré vectors $\mathbf{q}^*_{m1}$ and $\mathbf{q}^*_{m2}$ is indicated. From the orientation of these vectors, it is possible to determine the orientation of the substrate by comparing it with Fig. 2(c). This confirms the relations between the orientations of the substrate and the film.

Images of the overlayer along the [111] direction reveal the orientation differences of neighboring grains (Fig. 5). If it is then possible to determine the orientation of the substrate (by directly imaging the lattice or by using the moiré fringes) we can measure the rotation angle θ for the different domains. For both C_{60} and C_{70} films, rotated domains have been observed, although these grains were very small and rather exceptional in the case of C_{60}. Where it was possible to determine the orientation of the underlying substrate, the rotation angle θ was measured and included in Table I. This method is most sensitive and accurate for relatively large rotation angles, although $\theta\approx2°$ was also observed for C_{70} films, similar to the ED results. All observed domain boundaries are ''smeared out'' over a several molecule diameters wide region. In some cases [Figs. 5(a) and 5(c)] a moiré pattern in this transition region is observable, indicating that the domain boundary is inclined with respect to the substrate surface or is not planar. Furthermore, the boundaries are not along well-defined crystallographic directions although it is impossible to determine the structure of the domain edges at the level of the first monolayer.

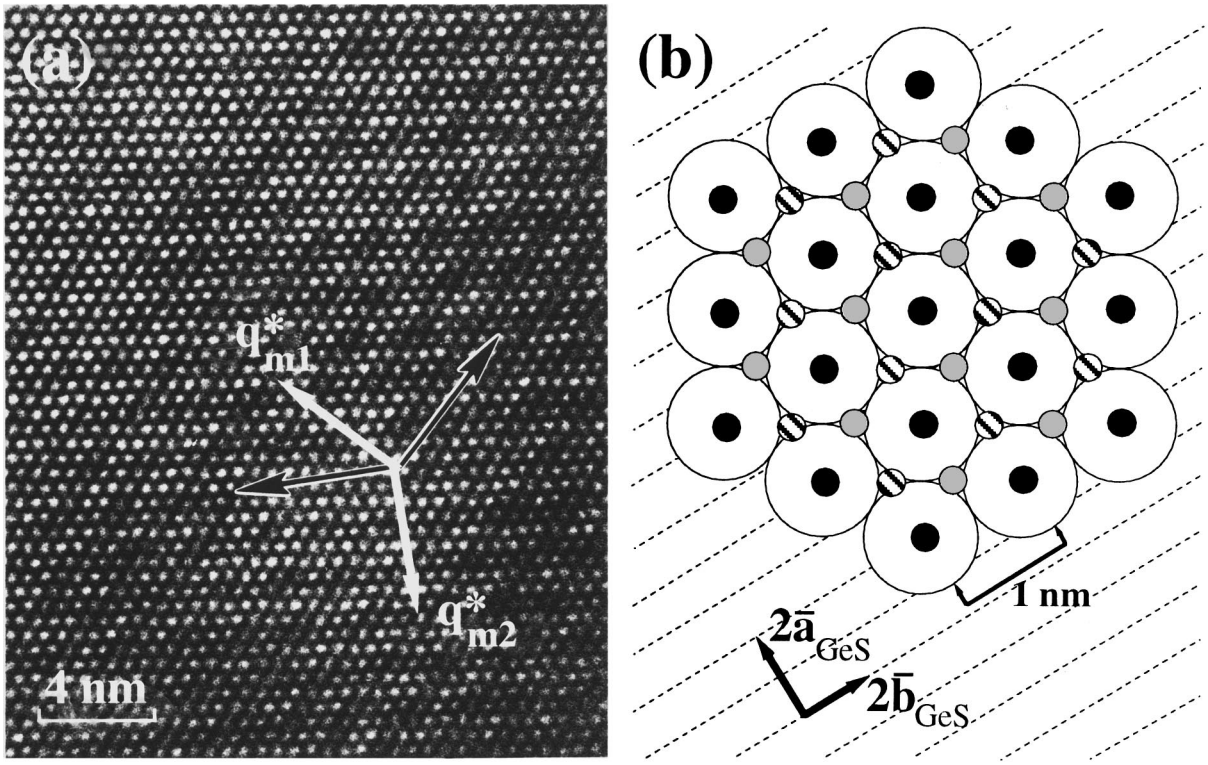

FIG. 4. (a) [111] high resolution (HREM) image of a C_{60} overlayer on GeS (001). By looking along the dark arrows, the moire fringes become visible. The direction of the corresponding moiré-vectors is also indicated (perpendicular to the fringes). These vectors are also indicated in Fig. 2(c). (b) Schematic representation of the first monolayer of C_{60} molecules on the GeS (001) surface. The centers of the molecules are indicated by black dots, while the projected positions of the centers of the molecules of the second and the third layers are also indicated.

Downloaded¬05¬Aug¬2009¬to¬192.38.67.112.¬Redistribution¬subject¬to¬AIP¬license¬or¬copyright;¬see¬http://jap.aip.org/jap/copyright.jsp

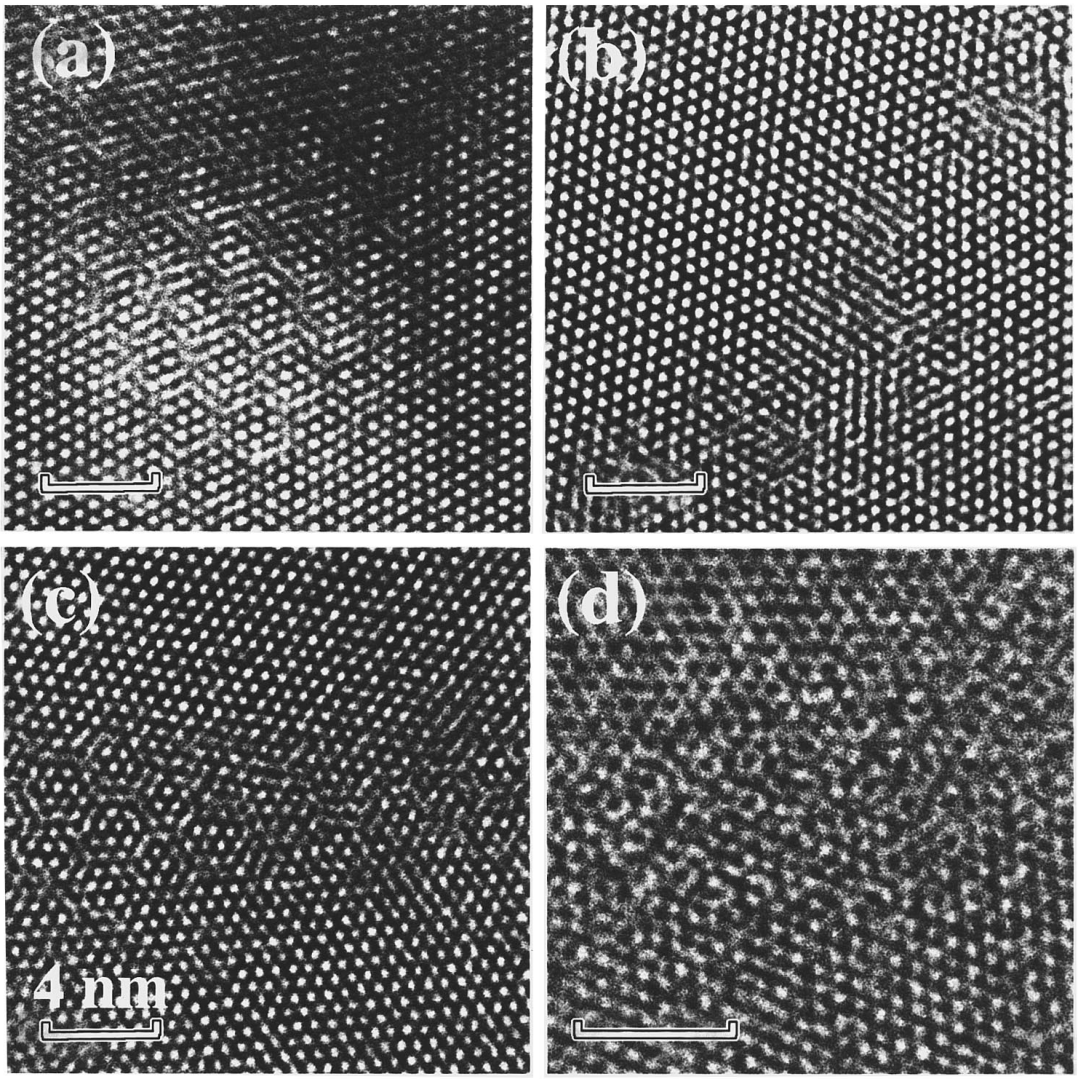

FIG. 5. [111] HREM images of domain boundaries in C_{60} [(a), (b), and (c)] and C_{70} (d) films. In (d), one part is oriented on the substrate according to orientation I, while the other part adopts orientation II. The scale bars indicate 4 nm.

Another type of domain boundary, unknown for bulk C_{60} or C_{70} crystals, observed in both C_{60} and C_{70} overlayers is shown in Fig. 6. The orientation of the underlying substrate was determined, using moiré fringes. The grains on both sides of the boundary have the same orientation, but are slightly translated with respect to each other. The grain boundary is parallel to the [110] direction of the C_{60} layer. Occasionally the boundary was observed to make a kink of 60°, thus following another close-packed [110] row of C_{60} molecules [Fig. 6(b)]. In the previous paragraph we mentioned that the close packed [101] rows of C_{60} molecules were perfectly aligned with the one-dimensional grooves in the substrate surface, hereby systematically skipping every second. By numbering the grooves, only the even numbered grooves are occupied by some domains and the odd numbered grooves by others; domain walls will be formed where the domains join. The resulting translation vector $\mathbf{\Delta}$ can be described in terms of the lattice vectors of the substrate: $\mathbf{\Delta}=\overline{\mathbf{a}}+x\mathbf{b}$. A value for x consistent with the images is $x=-0.266$ (the minus sign indicates that the structure is shifted towards the domain boundary) for which the minimal distance between the centers of the molecules in the first monolayer of the domains is 1 nm, the normal C_{60}–C_{60} distance for the bulk material. The resulting structure of the first monolayer is shown schematically in Fig. 7. Grain boundaries, both in the plane normal to the substrate surface or inclined were observed. The possible existence of this kind of defect was already proposed by Gensterblum *et al.*[18]

During the growth of the overlayer, several domains nucleate on the GeS surface and the first monolayer is progressively completed. The nucleation sites (odd or even grooves) of the domains determine whether different domains can join, or alternatively a domain boundary will be formed. The formation of a boundary will only occur if it is rather difficult for the molecules to move from one groove into another. However, the fact that the smallest distance between molecules of both domains is close to 1 nm, the normal distance for C_{60}, suggests that the C_{60} molecules can move easily parallel to the *b* axis of GeS, i.e., within one groove.

Downloaded¬05¬Aug¬2009¬to¬192.38.67.112.¬Redistribution¬subject¬to¬AIP¬license¬or¬copyright;¬see¬http://jap.aip.org/jap/copyright.jsp

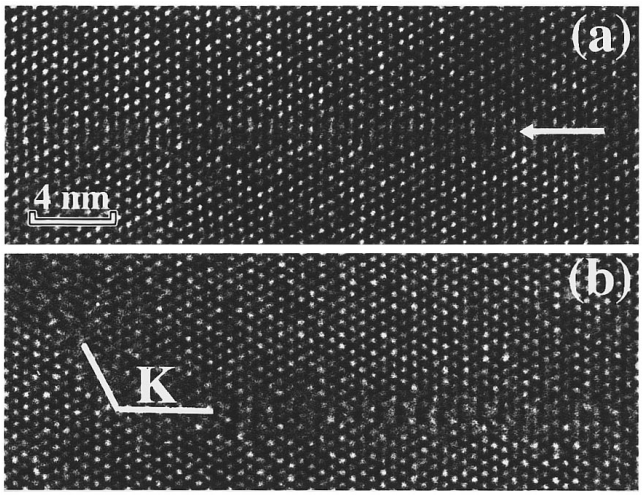

FIG. 6. [111] HREM image of translational domain boundaries in C_{60}. In (b), the domain boundary has a kink of 60° on K.

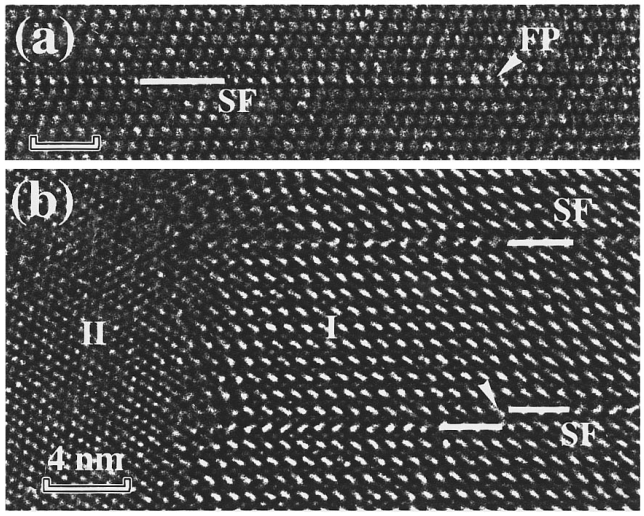

FIG. 8. [011] image of C_{60} film. (a) A Frank partial (FP) and its associated stacking fault (SF). In (b) a stepped stacking fault (arrow) is visible. Part I is imaged along the [011] direction; grain II is shown along the [114] zone.

2. ⟨011⟩ zones of the substrate

HREM images taken along a ⟨011⟩ zone-axis parallel to the substrate surface would show the stacking of the close-packed layers on the substrate surface, but require cross-section samples. Images taken along inclined ⟨011⟩ zones show the stacking of close-packed layers which are inclined with respect to the substrate surface. Most defects commonly observed in bulk C_{60} or C_{70} crystals, i.e., coherent (micro-) twin boundaries and stacking faults, were found to exist in the C_{60} and C_{70} overlayers on GeS. Figure 8(a) shows a Frank partial dislocation and its associated stacking fault and in Fig. 8(b) a stepped stacking fault is visible (arrow), which results in the formation of a dipole of stair-rod dislocations.[42] In Fig. 8(b) we can observe regions with different image detail. The pattern of bright dots in region I is very similar to the simulated pattern shown in Fig. 3 of Ref. 42 for a crystal thickness of ~5 nm and a defocus value of −60 nm. However, the dot pattern in part II is much denser but the rows of dots are continuous across the intermediate region. The pattern of region II does not correspond to any of the simulated images and thus cannot be attributed to a variation in thickness or defocus. However, the pattern is very similar to images obtained for crystals of cagelike silicon structures recently observed by TEM.[43] Part I corresponds to the [011] image of the C_{60} crystal, while part II is an image of a [114] zone. These images occur when there is a coherent twin present in the stacking of the {111} planes which are not parallel to the [011] direction.[43] The continuous transition between the two types of patterns is caused by the overlapping [011] and [114] patterns and by the inclination of the twin interface with respect to the electron beam.

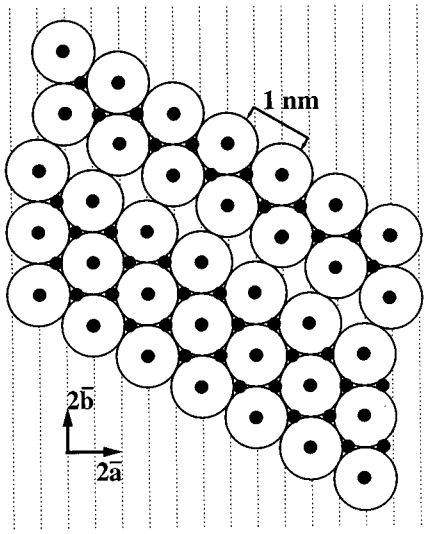

FIG. 7. Schematic representation of the domain boundary shown in Fig. 6. The dark dots indicate the positions of the spots visible in the HREM image.

IV. DISCUSSION

Fullerene films grown on different substrates were frequently observed to be rotated on the surface of the substrate. The preference for specific rotation angles of fullerene films grown on heated glass was attributed to the high symmetry grain boundaries present for these orientations.[44] The rotation angles were only determined by the symmetry of the overlayer and not influenced by the substrate. For the much larger grains in the epitaxially grown films this effect becomes less important and the orientation of the overlayer is determined by the substrate. However, even for these large grains, small misalignments with the substrate were observed. This was attributed to the relatively large misfit between the lattice parameters of the overlayer and the substrate,[19,30] but was never studied in detail.

The rotation angles θ observed for C_{60} and C_{70} films grown on GeS (001) are summarized in Table I. Only specific rotation angles were observed, especially $\theta \approx 2°$ in C_{70}. For C_{60}, only in exceptional cases was a small rotated domain observed; the majority of C_{70} domains was slightly rotated.

Downloaded¬05¬Aug¬2009¬to¬192.38.67.112.¬Redistribution¬subject¬to¬AIP¬license¬or¬copyright;¬see¬http://jap.aip.org/jap/copyright.jsp

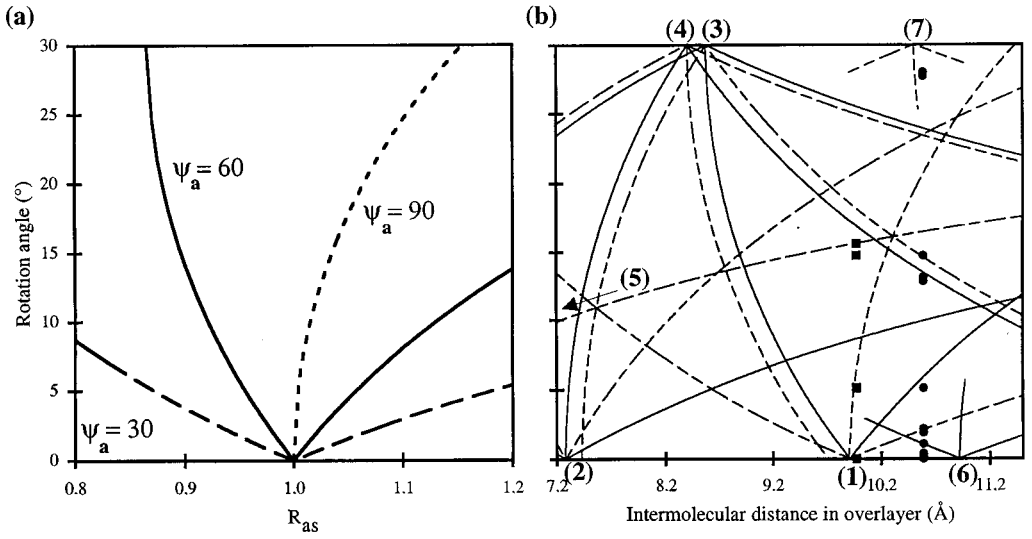

FIG. 9. (a) Rotation angle θ as a function of lattice misfit R_{as} for $\Psi_a = 30°$, 60°, and 90° solutions of the symmetry principle for epitaxial rotation. (b) Predicted and observed rotation angles for a hexagonal overlayer on the GeS (001) surface as a function of the intermolecular distance in the overlayer. The commensurate structures used are numbered. Full lines are the solutions for grains with {10}-facets (facets parallel to a ⟨110⟩ direction), while the dashed lines correspond to grains with {11} facets (parallel to a ⟨112⟩ direction). The small rectangles indicate the observed rotation angles for C_{60} grains, while the circles correspond to observations on C_{70} films (Table I).

The existence of epitaxial rotation is known in a number of different systems.[45] A very simple model was proposed by Grey *et al.*,[36] predicting rotation angles for a specific film and substrate, by starting only from simple symmetry considerations. This symmetry principle states that the energy of a finite overlayer on an infinite substrate is (locally) minimal if the moiré-vectors $\mathbf{q}_m$ (difference between a reciprocal vector $\mathbf{q}_a$ of the adsorbate and $\mathbf{q}_s$ of the substrate surface) are perpendicular to the facets or defects in the overlayer (Ψ_a solutions) or perpendicular to for example surface steps in the substrate (Ψ_s solutions).[46]

We define $r_{as} = q_s/q_a$ and $r_{sa} = 1/r_{as}$, depending on the lattice mismatch between substrate and film. The angle θ between $\mathbf{q}_s$ and $\mathbf{q}_a$ as a function of r_{sa} and Ψ_a, the angle between the moiré vector $\mathbf{q}_m$ and $\mathbf{q}_a$, is given by:[36]

$$\cos\,\theta = r_{sa}\,\sin^2\,\Psi_a + \cos\,\Psi_a \sqrt{1 - r_{sa}^2\,\sin^2\,\Psi_a}, \tag{1}$$

or as a function of r_{as} and Ψ_s (angle between $\mathbf{q}_m$ and $\mathbf{q}_s$) by

$$\cos\,\theta = r_{as}\,\sin^2\,\Psi_s + \cos\,\Psi_s \sqrt{1 - r_{as}^2\,\sin^2\,\Psi_s}. \tag{2}$$

According to the symmetry principle, the moiré vector will be preferentially perpendicular to the overlayer facets or to defects on the substrate surface which are mostly found along high-symmetry directions of the film and substrate; therefore high symmetry angles for Ψ_a and Ψ_s are of interest (for the hexagonal C_{60} and C_{70} films, Ψ_a is 0°, 30°, 60°, or 90°; for the rectangular GeS (001) surface Ψ_s is 0°, 40° (if $\mathbf{q_s} = \mathbf{b}^*$), 50° (if $\mathbf{q_s} = \mathbf{a}^*$) or 90°). Values for θ as a function of r_{as} for the high symmetry angles are shown in Fig. 9(a).

Different $\mathbf{q_a}$ vectors can be compared with different $\mathbf{q_s}$ vectors, and if $\mathbf{q_a}$ matches with $\mathbf{q_s}$ (both in length and direction), a commensurate structure is formed. For all such cases, one can define r_{as} and the pattern of solutions shown in Fig. 9(a) starts at every commensurate structure. The first type of commensurate structure occurs whenever the distance between the molecules of the overlayer fits n times (n integer) a lattice parameter of the surface while a second type occurs when the distance between rows of molecules fits a lattice parameter of the substrate. Only some of the commensurate structures are fundamentally commensurate (each atom of the unrelaxed adsorbate layer can be placed in a minimum of the substrate potential).[46] In this way we arrive at Fig. 9(b) where the expected low energy configurations for a hexagonal overlayer on a rectangular GeS (001) surface are plotted as a function of the lattice parameter and the rotation angle of the overlayer and for overlayers with facets parallel to a ⟨110⟩ direction ({01} facets for the first monolayer) (full lines), and facets parallel to a ⟨112⟩ direction ({11} facets) (dashed lines). Only Ψ_a solutions are plotted. Commensurate structures (1), (4), (5), and (7) correspond to structures of the second type (distance between rows are $2a$, $2b$, a and $5/3b$, respectively); numbers (2), (3), and (6) are of the first type (distance between molecules is $2b$, $2a$, and $3b$, respectively). Structures (1)–(5) are fundamentally commensurate.

Numerical simulations[36] were carried out for the rectangular GeS (001) substrate. The interface energy E of an overlayer with N molecules on positions (x_i, y_i) was calculated as a function of the lattice parameter of the overlayer and of the adsorbate rotation by the equation

$$E(N,\phi) = \sum_{i=1}^{N} \cos\left(\frac{2\pi}{a}\,(x_i + \phi_x)\right) + \cos\left(\frac{2\pi}{b}\,(y_i + \phi_y)\right). \tag{3}$$

Only the first Fourier components of the substrate potential are used. The energy was minimized with respect to the reg-

Downloaded¬05¬Aug¬2009¬to¬192.38.67.112.¬Redistribution¬subject¬to¬AIP¬license¬or¬copyright;¬see¬http://jap.aip.org/jap/copyright.jsp

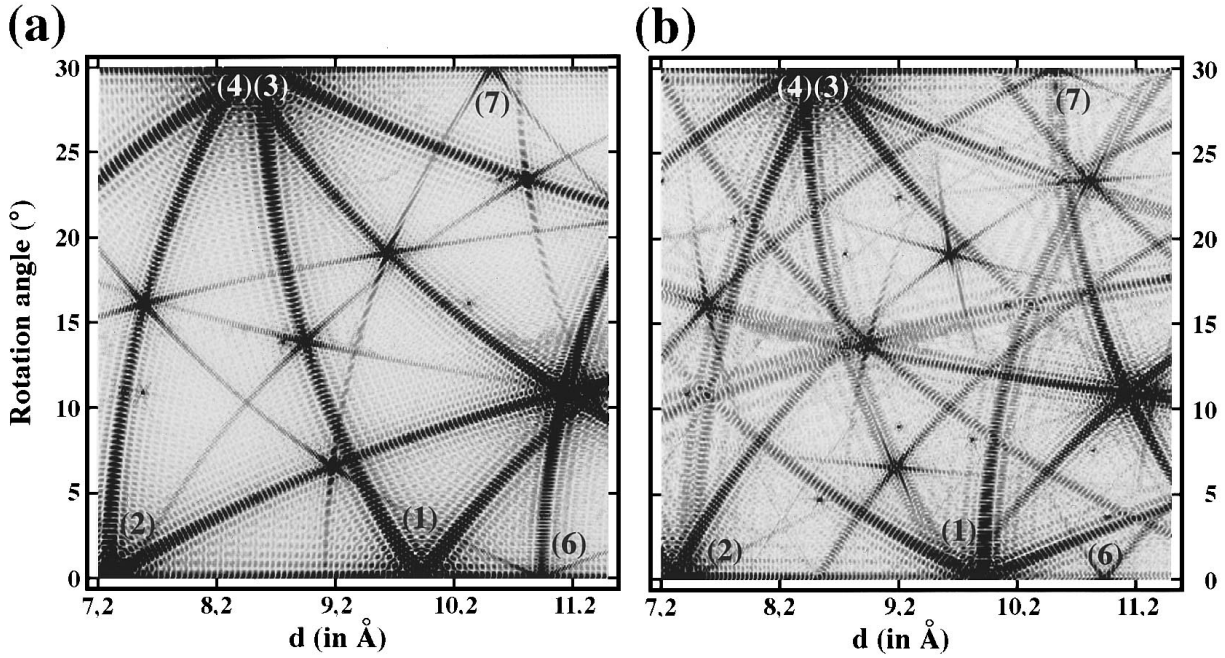

FIG. 10. Interface energy simulation [on GeS (001)] for hexagonal overlayers with {10} (a) and {11} (b) facets as a function of rotation angle and intermolecular distance in the overlayer. The dark regions are low energy configurations. Elastic effects were incorporated in the model and yielded extra commensurate structures and the appearance of the smaller low energy lines.

istry $\phi=(\phi_x,\phi_y)$.[36] Some elastic relaxation of the overlayer molecules on the GeS surface was incorporated in the calculations using the same simple approximation as in Ref. 36. The results for overlayers with {10} and {11} facets are plotted in Figs. 10(a) and 10(b), respectively. Comparison of Figs. 10(a) and 10(b) with Fig. 9(b) shows that the symmetry principle can be perfectly applied for hexagonal films on a rectangular surface. Each line in Fig. 9(b) originates from one or more commensurate structures. As not all commensurate structures have been considered, some of the low energy solutions in Figs. 10(a) and 10(b) do not appear in Fig. 9(b).

Observed rotation angles for C_{60} and C_{70} are indicated in Fig. 9(b). Most of the points lie within experimental error (indicated in Table I) on a low energy line. The observed preference of C_{70} grains to be rotated over 2° is particularly significant because this is the expected solution if we consider the substrate surface as a collection of parallel one-dimensional grooves (2.06° for $\Psi_a=30°$). Solutions are found for grains with {10} and {11} facets; for some observed angles it is necessary to incorporate elastic effects [structures (6) and (7)]. Although most observed angles can be found by comparing the lattice parameter of the film with the *a* parameter of GeS, some angles can only be reproduced by comparison with the *b* parameter; the model of the parallel one-dimensional grooves for the substrate surface is thus oversimplified.

There are several conceivable physical mechanisms which can cause epitaxial rotation, all of which would lead to the high symmetry solutions of Fig. 9(b). The rotation angle alone is not enough to elucidate the physical origin of the rotation. Examples of possible causes of epitaxial rotation are energy minimization due to elastic effects, due to defects within the adsorbate layer or due to the facet structure of the initial nuclei of the film. Compared to the widely studied case of epitaxial rotation in monolayer films, there is the further complication of the multilayer nature of the present adsorbate. Experiments carried out in the early stages of growth, when the grains of the first monolayer are still separated, are necessary to determine whether the epitaxial rotation is caused by the facets of the grains, the presence of defects in the film, or by elastic effects. The observations of the higher fullerenes films (e.g., C_{76}, fcc with lattice parameter 1.53 nm) on the GeS surface could be an extra test for the symmetry model. An expected rotation angle for this film would be 2.7° which corresponds to the 2.06° solution for C_{70}.

V. CONCLUSION

HREM images and ED patterns were used to study the structural characteristics of epitaxial C_{60} and C_{70} films grown on a GeS (001) surface. The observations confirm the very good quality of the C_{60} films. The quality of the C_{70} films is, although still remarkably high, much lower. Stacking faults and microtwins, commonly observed in bulk fullerene crystals, are present in the overlayers. The presence of grain boundaries between domains occupying odd and even numbered grooves on the substrate surface implies that the fullerene molecules align easily along these one-dimensional grooves, but cannot move from one groove into another. Furthermore, the rotation of the overlayer domains, mostly observed in C_{70} films, but sporadically also in C_{60}, was attributed to the difference in lattice parameter between substrate and overlayer. A simple symmetry model was numerically tested for the present configuration and used for explaining the observed rotation angles. It was found that the approxi-

Downloaded¬05¬Aug¬2009¬to¬192.38.67.112.¬Redistribution¬subject¬to¬AIP¬license¬or¬copyright;¬see¬http://jap.aip.org/jap/copyright.jsp

mation of the substrate surface by one-dimensional grooves in which the molecules can move freely, is oversimplified and that the periodicity along these grooves, as well as elastic effects in the overlayer play a role in the determination of the arrangement of the molecules on the surface.

ACKNOWLEDGMENTS

The authors acknowledge critical reading of the manuscript by J. Van Landuyt and P. A. Thiry. This text presents research results of the Belgian Programme on InterUniversity Poles of Attraction initiated by the Belgian State, Prime Minister's Office of Science Policy Programming (Federal Services of Scientific, Technical and Cultural Affairs) and by the Wallonia region. The scientific responsibility is assumed by the authors. K. Hevesi is grateful to the FRIA for financial support.

[1] H. W. Kroto, J. R. Heath, S. C. O'Brien, R. F. Curl, and R. E. Smalley, Nature **318**, 162 (1985).
[2] W. Kratschmer, L. D. Lamb, K. Fostiropoulos, and D. R. Huffman, Nature **347**, 354 (1990).
[3] J. E. Rowe, P. Rudolf, L. H. Tjeng, R. A. Malic, G. Meigs, C. T. Chen, J. Chen, and E. W. Plummer, Int. J. Mod. Phys. B **6**, 325 (1992).
[4] T. Hashizume, K. Motai, X. D. Wang, H. Shinohara, Y. Saito, Y. Maruyama, K. Ohno, Y. Kawazoe, Y. Nishina, H. W. Pickering, Y. Kuk, and T. Sakurai, Phys. Rev. Lett. **71**, 2959 (1993).
[5] K. Motai, T. Hashizume, H. Shinohara, Y. Saito, H. W. Pickering, Y. Nishina, and T. Sakurai, Jpn. J. Appl. Phys. **32**, L450 (1993).
[6] J. K. Gimzewski, S. Modesti, and R. R. Schlittler, Phys. Rev. Lett. **72**, 1036 (1994).
[7] P. Rudolf *et al.* (private communication).
[8] E. I. Altman and R. J. Colton, Surf. Sci. **279**, 49 (1992).
[9] E. I. Altman and R. J. Colton, Phys. Rev. B **48**, 18244 (1993).
[10] J. K. Gimzewski, S. Modesti, Ch. Gerber, and R. R. Schlittler, Chem. Phys. Lett. **213**, 401 (1992).
[11] Y. Kuk, D. K. Kim, Y. D. Sub, K. H. Park, H. P. Noh, S. J. Oh, and S. K. Kim, Phys. Rev. Lett. **70**, 1948 (1993).
[12] X.-D. Wang, T. Hashizume, H. Shinohara, Y. Saito, Y. Nishina, and T. Sakurai, Phys. Rev. B **47**, 15923 (1993).
[13] H. Xu, D. M. Chen, and W. N. Creager, Phys. Rev. Lett. **70**, 1850 (1993).
[14] A. V. Hamza and M. Balooch, Chem. Phys. Lett. **201**, 404 (1993).
[15] Y. Z. Li, J. C. Patrin, M. Chander, J. H. Weaver, L. P. F. Chibante, and R. E. Smalley, Science **252**, 547 (1991).
[16] Y. Z. Li, M. Chander, J. C. Patrin, J. H. Weaver, L. P. F. Chibante, and R. E. Smalley, Phys. Rev. B **45**, 13837 (1992).
[17] J. H. Weaver, Acc. Chem. Res. **25**, 143 (1992).
[18] G. Gensterblum, L. -M. Yu, J. -J. Pireaux, P. A. Thiry, R. Caudano, J. -M. Themlin, S. Bouzidi, F. Coletti, and J. -M. Debever, Appl. Phys. A **56**, 175 (1993).
[19] B. J. Benning, F. Stepniak, and J. H. Weaver, Phys. Rev. B (1979–Present) **48**, 9086 (1993).
[20] Y. Z. Li, J. C. Patrin, M. Chander, J. H. Weaver, K. Kikuchi, and Y. Achiba, Phys. Rev. B **47**, 10867 (1993).
[21] G. Gensterblum, K. Hevesi, B.-Y. Han, L. -M. Yu, J. -J. Pireaux, P. A. Thiry, R. Caudano, A.-A. Lucas, D. Bernaerts, S. Amelinckx, G. Van Tendeloo, G. Bendele, T. Buslaps, R. L. Johnson, M. Foss, R. Feidenhans'l, and G. LeLay, Phys. Rev. B **50**, 11981 (1994).
[22] M. Sakurai, H. Tada, K. Saiki, A. Koma, H. Funasaka, and Y. Kishimoto, Chem. Phys. Lett. **208**, 425 (1993).
[23] G. Gensterblum, L.-M. Yu, J.-J. Pireaux, P. A. Thiry, R. Caudano, Ph. Lambin, A. A. Lucas, W. Kratschmer, and J. E. Fischer, J. Phys. Chem. Solids **53**, 1427 (1992).
[24] M. Sakurai, H. Tada, K. Saiki, and A. Koma, Jpn. J. Appl. Phys. **30**, L565R (1991).
[25] K. Tanigaki, S. Kuroshima, J. Fujita, and T. W. Ebbesen, Appl. Phys. Lett. **63**, 2351 (1993).
[26] B. Y. Han, K. Hevesi, L. M. Yu, G. Gensterblum, P. A. Thiry, J.-J. Pireaux, and R. Caudano, J. Vac. Sci. Technol. A **13**, 1036 (1995).
[27] D. Schmicker, S. Schmidt, J. G. Skofronick, J. P. Toennies, and R. Vollmer, Phys. Rev. B **44**, 10995 (1991).
[28] H. G. Busmann, R. Hiss, H. Gaber, and I. V. Hertel, Surf. Sci. **289**, 381 (1993).
[29] W. Krakow, N. M. Rivera, R. A. Roy, R. S. Ruoff, and J. J. Cuomo, Appl. Phys. A **56**, 185 (1993).
[30] J. E. Fischer, E. Werwa, and P. A. Heiney, Appl. Phys. A **56**, 193 (1993).
[31] W. B. Zhao, X. D. Zhang, Z. Y. Ye, J. L. Zhang, C. Y. Li, D. L. Yin, Z. N. Gu, X. H. Zhou, and Z. X. Jin, Solid State Commun. **85**, 311 (1993).
[32] H.-G. Busmann, R. Hiss, H. Gaber, and I. V. Hertel, Surf. Sci. **289**, 381 (1993).
[33] W. B. Zhao, X. D. Zhang, Z. Y. Ye, J. L. Zhang, C. Y. Li, D. L. Yin, Z. N. Gu, X. H. Zhou, and Z. X. Jin, Thin Solid Films **240**, 14 (1994).
[34] N. Tanaka, T. Kitagawa, T. Kachi, and T. Kizuka, Ultramicroscopy **52**, 533 (1993).
[35] Y. Z. Li, J. C. Patrin, M. Chander, J. H. Weaver, K. Kikuchi, and Y. Achiba, Phys. Rev. B **47**, 10867 (1993).
[36] F. Grey and J. Bohr, *Phase Transitions in Surface Films 2*, edited by H. Taub (Plenum, New York, 1991); F. Grey and J. Bohr, Europhys. Lett. **18**, 717 (1992); F. Grey and J. Bohr, Appl. Surf. Sci. **65/66**, 35 (1993).
[37] K. Hevesi (private communication).
[38] I. Rusakova, A. Hamed, and P. H. Hor, J. Mater. Res. **9**, 2814 (1994).
[39] See, P. A. Gravil, Ph. Lambin, G. Gensterblum, L. Henrard, A. A. Lucas, and P. Senet, Surf. Sci. **329**, 199 (1995). The C_{60} molecules are probably more stable on top of the ''hills'' and not at the bottom of the grooves. From our observations it is impossible to distinguish between both situations, and it does not change the reasoning made in the following parts of the paper.
[40] M. A. Verheijen, H. Meekes, G. Meijer, P. Bennema, J. L. de Boer, S. van Smaalen, G. Van Tendeloo, S. Amelinckx, S. Muto, and J. Van Landuyt, Chem. Phys. **166**, 287 (1992).
[41] G. Van Tendeloo, S. Amelinckx, J. L. de Boer, S. Van Smaalen, M. A. Verheijen, H. Meekes, and G. Meijer, Europhys. Lett. **21**, 329 (1993).
[42] S. Muto, G. Van Tendeloo, and S. Amelinckx, Philos. Mag. B **67**, 443 (1993).
[43] L. Nistor, G. Van Tendeloo, S. Amelinckx, and C. Cros, Phys. Status Solidi A **146**, 119 (1994).
[44] Y. Takahashi, Jpn. J. Appl. Phys. **33**, 4104 (1994).
[45] A. D. Novaco and J. P. McTague, Phys. Rev. Lett. **38**, 1286 (1977); J. P. McTague and A. D. Novaco, Phys. Rev. B **19**, 5299 (1979).
[46] J. Bohr and F. Grey, Condens. Matter News **1**, 12 (1992).

Downloaded¬05¬Aug¬2009¬to¬192.38.67.112.¬Redistribution¬subject¬to¬AIP¬license¬or¬copyright;¬see¬http://jap.aip.org/jap/copyright.jsp